Double-differential cross sections for single ionization of simple polyatomic molecules by proton impact

A. Mondal,[1] S. Halder,[2] S. Mukherjee,[2] C. R. Mandal,[2] and M. Purkait[2,*]
[1]*Department of Physics, Ramsaday College, Amta, Howrah 711401, India*
[2]*Department of Physics, Ramakrishna Mission Residential College, Narendrapur, Kolkata 700103, India*
(Received 23 June 2017; revised manuscript received 14 August 2017; published 18 September 2017)

A theoretical study of double-differential cross sections (DDCSs) for single ionization of CH_4 and NH_3 molecules by collision with proton is presented at 0.25, 1, and 2 MeV, respectively. For the final state, we use a continuum distorted wave that contains the product of three-Coulomb distortion due to pairwise Coulombic interactions for which it is called the three-Coulomb wave model. In the entrance channel, the Coulomb distortion between the incoming projectile and the target is taken. In this model, the ground state of the polyatomic molecule is described by means of an accurate one-center molecular wave function, which is a linear combination of atomic orbitals. The contributions of DDCSs for different molecular orbitals of the polyatomic molecules to the spectrum of angular distributions at different electron emission energies have also been analyzed. Generally the preference for ionization depends on the binding energy of the active electron in molecular orbital in the ascending order of loosely bound electrons to more tightly bound electrons. At large ejected electron and projectile energy, the lesser bound electrons in the molecules dominate the DDCS at extreme forward emission angles. The present DDCS results are compared with available experimental and the theoretical findings. In case of ammonia molecules, good agreement is observed at all projectile energies, showing that the present model is sufficient to explain all the experimental data for double-differential cross sections. However, some degree of discrepancy is observed at 2 MeV proton impact for small electron emission angles when CH_4 molecular target is considered.

DOI: 10.1103/PhysRevA.96.032710

I. INTRODUCTION

It has been well known for a long time [1] that ionization of atoms and molecules by the impact of charged particles is of prime importance in a large number of areas such as plasma physics, astrophysics, radiation physics, and in the study of penetration of charge particles through matter. Recently, it has been shown that experimental and theoretical data about the ionization of biological molecules are needed in fundamental studies of the charged particle interaction in a biological system for which there is a need of the knowledge of cross sections concerning charge exchange and ionization processes originated by charged particle impact. In addition, it has been checked that ionization cross sections for biological molecules are quite useful in medical studies, such as radiobiology, medical imaging, and radiotherapy. One of the main difficulties for ionization of molecules is the multicenter character of the target wave function. Various inelastic processes explored for atomic targets, such as binary collision and two center effects (TCEs) [2–7] emerge for molecular collisions. However, the investigation of multicenter molecular targets provides the possibility of observing Young-type interference effects, especially in the case of homonuclear diatomic molecules.

It is well known that the Gaussian program [8,9] provides multicenter wave functions, which can be applied for description of the ground-state properties of molecular targets. However, for simple polyatomic molecules, single-center wave functions offer a realistic description of the initial states of the target molecules [10]. Theoretically, few models [11–15] have been proposed to study the double-differential cross sections (DDCSs) for single ionization of low-Z polyatomic molecules such as methane, ammonia, etc. using different molecular description for initial state of the target molecules. Single ionization of molecules involve three charged unbound particles in the final state: the scattered projectile, the ejected electron and the residual target ion. However, the long-range Coulomb force forbids the free motion of the particles even at infinite interparticle separation. So the final state consists of a three-body Coulomb continuum, which is a correlated one.

In this paper we consider the single ionization of methane and ammonia molecules by protons at high impact energies. The results are derived using an analytical expression for the transition amplitude in the frame work of three-Coulomb wave (3CW) model in the exit channel and the distortion between projectile target in the entrance channel, respectively.

Different sophisticated methods, such as the Brauner, Briggs, and Klar (BBK) model [16], called the three-Coulomb wave (3CW) model, the converged closed coupling (CCC) [17], or the exterior complex scaling method (ECS) [18], the continuum distorted wave eikonal-initial-state (CDW-EIS) [19], have been used to calculate the double-differential cross section (DDCS) for ion-impact ionization of molecules, which is computationally cumbersome. For molecules with chemical form XH_n, where X is a much heavier atom compared with the hydrogen atom, the molecular wave function can be expanded on basis set, all referring to one origin [20–23]. Senger [24] has calculated the molecular DDCS for single ionization of molecules by 0.25–2 MeV proton impact based on the plane-wave Born approximation with mixed treatment, called (DDCS-MT). Later, TCS and DDCS for single ionization of low-Z molecules (N_2, CO, CH_4, and CO_2) by proton impact have been calculated by applying the CDW-EIS model [25]. In that work [25], two different approximations have been chosen for molecular

*Corresponding author: mpurkait_2007@rediffmail.com; rkmcnpur@vsnl.com.

description. One of them is known as Bragg's additivity rule, which consists in expressing each molecular cross section as a linear combination of atomic cross sections weighted by the number of atoms in the molecules [26]. In the second one, called complete neglect of differential overlap (CNDO), the molecular orbitals are written in terms of atomic orbitals of the atomic constituents [27].

Champion *et al.* [28] have reported the differential and total ionization cross sections of polyatomic molecules (CH_4, NH_3, and H_2O) by fast electron impact. The calculation has been performed in the distorted wave Born approximation. In that work, the molecular target wave functions are described by linear combination of atomic orbitals (LCAO). The calculation shows very good agreement with the experimental measurements [29], but remain limited to triple-differential cross sections (TDCSs) at smaller electron emission angles. Differential and total cross sections for single ionization of large molecules (cytosine) by protons in the incident energy range of 0.1–100 MeV have been studied using the first Born approximation [30]. In that model, the ground-state wave function of the molecules is described by means of an accurate one-center molecular wave function. In their study, they have neglected the ionization of inner shell electrons, which have significant emission probability except for large values of ejected angles verified in a previous study [31].

A theoretical investigation of fully differential cross sections (FDCS) for the single ionization of CH_4 by collisions with bare ions (H^+, He^{2+}, and C^{6+}) has been performed by Menchero and Otranto [32] within the framework of Born distorted wave model called Born-3DW. In the final state, they considered a non-Coulombic central potential to represent the ionization of the emitted electron with the residual molecular ion. There is no experimental data available for comparison to test the validity of the theoretical model. However, ionization of methane molecule in collision with protons in the range of impact energies from 50 keV to 10 MeV has been investigated by applying the CDW-EIS approximation [33] extended for multicenter collisions. In these calculations, the continuum orbitals for the ejected electrons have been calculated on spherical asymmetric potentials constructed via the configuration of the initial state where the orthogonality criteria for the initial and final wave functions of the active electron is violated. We see that these results are sensitive to the value of the equilibrium C-H distance used in the construction of core potential of the molecule. The obtained results are in reasonable agrement with the experimental findings [24].

Yavuz *et al.* [34] have investigated the details of electron emission from a methane molecule by measuring the absolute electron DDCS at incident energies ranging from 50–350 eV and for a large number of ejection energies and angles. The measured data have been compared with their calculations in the first Born approximation-Coulomb wave (FBA-CW) model. The FBA-CW results are in good agreement with measurements at small ejection angles and ejection energies. DDCS for single ionization from NH_3 and CH_4 molecules by impact of protons have been calculated within the postform and prior form of the CDW-EIS model [35], considering either the Moccia representation or the molecular orbitals constructed from a LCAO in a self-consistent field (MO-LCAO-SCF). The discrepancies have been found when the CH_4 molecular target is considered.

Depending on the success of three-Coulomb wave model (3CW) [36,37] for ionization in ion-atom and/or ion-molecule collision, we are motivated to study the DDCS for the single ionization of CH_4 and NH_3 molecules in collision with protons in the framework of extended 3CW approximation in the incident energy range 0.25–2 MeV. Comparisons are made between the present results and their corresponding experimental values as well as the results obtained from other theories. In addition, the contributions of DDCS for five different molecular orbitals of CH_4 and NH_3 to the spectrum of angular distributions have also been analyzed.

The paper is organized as follows. The theory is described in Sec. II. Section III deals with a comparison of theoretical and experimental data in terms of DDCSs. Conclusions are given in Sec. IV. Atomic units are used throughout this work unless otherwise indicated.

II. THEORY

The DDCSs for single ionization presented in this paper are calculated within the framework of the three-Coulomb wave (3CW) model with distortion in the initial channel. Single ionization of molecules by proton impact may be written as

$$p + M \longrightarrow p + M^+ + e^-. \tag{1}$$

For this process, we present an extension of the three-Coulomb wave (3CW) model to describe the single ionization of molecules. As for atomic targets, the multielectronic problem has been reduced to a monoelectronic ion using the independent electron approximation where the multiparticle collision system may be reduced to a three-particle collision system consisting of the projectile (P), the active electron (e^-), and the residual target ion (M). It is assumed that the other electrons remain passive in the orbitals during the collision, which is valid at high impact energies. However, the occupied molecular orbitals for the initial state have been constructed by one-center molecular wave functions proposed by Moccio [20,21], which are described by the linear combination of atomic orbitals. In addition, the impact energies are so high that the collision time is several orders less than the relaxation time of both rotation and vibration of the molecules. It is possible to assume that the molecular nuclei remain fixed in their initial positions during the reaction. We consider that an incident proton (p) of charge Z_P ($Z_P = 1$ here) and initial momentum $\vec{k}_i$ ionizes a stationary target molecule. The final state of the system is then characterized by a scattered proton of momentum $\vec{k}_R$ and an ejected electron of the momentum $\vec{k}_e$.

The position vector of the electron with respect to the heaviest nucleus of the molecular target is $\vec{r}$ and with respect to the projectile is $\vec{s}$. Further, $\vec{R}$ denotes the position vector of the proton with respect to the same center. The prior transition amplitude for single ionization can be written as

$$T_{if} = \langle \psi_f | V_i | \psi_i \rangle, \tag{2}$$

where ψ_i is the initial channel wave function. Here we consider that the initial bound state of the target molecule is distorted

by the incoming projectile. However the distortion due to the interaction of the projectile ion with respect to the screened target, is described by the coulomb Continuum wave functions in the initial channel. Thus the initial channel wave function of the molecule ψ_i may be written as

$$\psi_i = (2\pi)^{-\frac{3}{2}} e^{-\frac{\pi}{2}\alpha_4}\Gamma(1+i\alpha_4)e^{i\vec{k}_i.\vec{R}}\,{}_1F_1 \times [-i\alpha_4;1;i(\vec{k}_i.\vec{R}-k_iR)]\Phi_M(\vec{r}), \quad (3)$$

where $\alpha_4 = \frac{z_T^{\text{eff}}-1}{k_i}$ and $\Phi_M(\vec{r})$ is the initial wave function of the molecular orbital. z_T^{eff} is the screened charge of the target, chosen in such a way that it reproduces the correct binding energy, $z_T^{\text{eff}} = (-2n^2\epsilon_i)^{\frac{1}{2}}$, where n refers to the principal quantum number of each atomic orbital component used in the molecular target description and ϵ_i is the corresponding binding energy [20,21].

We have used the molecular description proposed by Moccia [20,21] who has developed each molecular wave function, denoted by $\phi_M^j(\vec{r})$ in terms of Slater-like functions centered at a common origin, mainly upon the heaviest nucleus, i.e., the carbon atom for CH_4 and the nitrogen atom for NH_3, respectively. The ten bound electrons in the CH_4 molecule are distributed among five one-center molecular wave function $\phi_M^j(\vec{r})$ with j ranging from 1–5 corresponding to the orbitals $1A_1$, $2A_1$, $1T_{2z}$, $1T_{2x}$, and $1T_{2y}$ whose binding energies are 11.195, 0.9204, 0.5042, 0.5042, and 0.5042 a.u., respectively. Similarly for the NH_3 molecule, the few orbitals are $1A_1, 2A_1, 3A_1\ 1E_x$, and $1E_y$ with bindings energies 15.522, 1.1224, 0.4146, 0.5956, and 0.5956 a.u., respectively. Each orbital is expressed by linear combinations of Slater-type functions, which can be written as

$$\phi_M^j(\vec{r}) = \sum_{k=1}^{N} a_{jk}\chi_{n_{jk}l_{jk}m_{jk}}(\vec{r}) \quad (4)$$

with

$$\chi_{n_{jk}l_{jk}m_{jk}}(\vec{r}) = R^{\xi_{jk}}_{n_{jk}l_{jk}(\vec{r})}(\vec{r})Y_{l_{jm}m_{jk}}(\hat{r})$$

$$\text{and} \quad R^{\xi_{jk}}_{n_{jk}l_{jk}}(\vec{r}) = \frac{(2\xi_{jk})^{n_{jk}+\frac{1}{2}}}{\sqrt{(2n_{jk})!}} r^{(n_{jk}-1)} e^{-\xi_{jk}r}.$$

Here N is the number of Slater-type orbitals used in the expansion of the jth molecular orbital and a_{jk} is the corresponding weights [28]. The initial perturbation potential V_i is obtained by subtracting the asymptotic potential from the total integration potential between the projectile and the target. So in the initial channel interaction V_i decreases much faster than the Coulomb potential at large internuclear distance. Thus V_i can be written as

$$V_i = \frac{Z_T^{\text{eff}}}{R} - \frac{1}{s} - \frac{\left(Z_T^{\text{eff}}-1\right)}{R} = \frac{1}{R} - \frac{1}{s}. \quad (5)$$

We have used one of the most sophisticated models, called the BBK model [16], which describes the final state by

$$\psi_f = (2\pi)^{-3}C_1 e^{i\vec{k}_e.\vec{r}}\,{}_1F_1[-i\alpha_1;1;-i(\vec{k}_e.\vec{r}+k_er)]C_2 e^{i\vec{k}_R.\vec{R}}\,{}_1F_1 \times [-i\alpha_2;1;-i(\vec{k}_s.\vec{s}+k_ss)]C_3\,{}_1F_1 \times [i\alpha_3;1;-i(\vec{k}_R.\vec{R}+k_RR)], \quad (6)$$

where $C_1 = e^{\frac{\pi}{2}\alpha_1}\Gamma(1+i\alpha_1)$, $C_2 = e^{\frac{\pi}{2}\alpha_2}\Gamma(1+i\alpha_2)$, $C_3 = e^{\frac{\pi}{2}\alpha_3}\Gamma(1-i\alpha_3)$ with $\alpha_1 = \frac{Z_T^{\text{eff}}}{k_e}$, $\alpha_2 = \frac{1}{k_s}$, $\alpha_3 = \frac{Z_T^{\text{eff}}}{k_R}$. In the final state, the charge of the residual target seen by the scattered proton and the ejected electron are also defined as the effective charge with $Z_T^{\text{eff}} = 1$ [38]. For this model, we have the well-known asymptotically correct Coulomb three-body wave function for the ejected electron and the scattered proton in the field of the residual ion. Here the relative wave vector between the scattered proton and the ejected electron is given by $\vec{k}_s = \vec{k}_R - \vec{k}_e$. Finally, the transition amplitude for single ionization in the present model may be written as

$$T_{if} = C(2\pi)^{-\frac{9}{2}}\sum_{j=1}^{5}\iint d\vec{r}d\vec{R}e^{i(\vec{k}_i-\vec{k}_R).\vec{R}-i\vec{k}_e.\vec{r}}\,{}_1F_1 \times [-i\alpha_4;1;i(\vec{k}_i.\vec{R}-k_iR)]\left(\frac{1}{R}-\frac{1}{S}\right){}_1F_1 \times [i\alpha_1;1;i(\vec{k}_e.\vec{r}+k_er)]_1F_1[i\alpha_2;1;i(\vec{k}_s.\vec{s}+k_ss)]_1F_1 \times [-i\alpha_3;1;i(\vec{k}_R.\vec{R}+k_RR)]\phi_M^j(\vec{r}), \quad (7)$$

where $C = e^{\frac{\pi}{2}(\alpha_1+\alpha_2-\alpha_3-\alpha_4)}\Gamma(1-i\alpha_1)\Gamma(1-i\alpha_2)\Gamma(1+i\alpha_3)\Gamma(1+i\alpha_4)$,
and the integral representation of confluent hypergeometric function may be written as

$${}_1F_1(i\alpha;1;Z) = \frac{1}{2\pi i}\oint_{\Gamma}^{0^+,1^+} P(\alpha,t)e^{zt}dt. \quad (8)$$

Here $P(\alpha,t) = t^{i\alpha-1}(t-1)^{-i\alpha}$, $P(\alpha,t)$ is single valued and analytic over the contour Γ enclosing 0 and 1 once anticlockwise, having a branch cut from 0 to 1. Using the integral representation of equation (8) [39], Eq. (7) may be written as

$$T_{if} = (2\pi)^{-\frac{9}{2}}\frac{C}{(2\pi i)^4}\sum_{j=1}^{5}\lim_{\epsilon_1,\lambda_1\to 0}\left(\frac{\partial^2}{\partial\lambda\partial\xi_{jk}} - \frac{\partial^2}{\partial\epsilon_1\partial\xi_{jk}}\right) \times \oint_{\Gamma_1}P(\alpha_1,t_1)dt_1\oint_{\Gamma_2}P(\alpha_2,t_2)dt_2 \times \oint_{\Gamma_3}P(\alpha_3,t_3)dt_3\oint_{\Gamma_4}P(\alpha_4,t_4)dt_4J, \quad (9)$$

where

$$J = \iint d\vec{r}d\vec{R}e^{i[(\vec{k}_i-\vec{k}_R)+\vec{k}_Rt_3+\vec{k}_it_4-\vec{k}_st_2].\vec{R}}e^{i[\vec{k}_et_1+\vec{k}_st_2-\vec{k}_e].\vec{r}} \times \frac{e^{-\beta_1 r}}{r}\frac{e^{-\lambda s}}{s}\frac{e^{-\epsilon R}}{R} \quad (10)$$

with $\beta_1 = \xi_{jk} - ik_et_1$, $\lambda = \lambda_1 - ik_st_2$, $\epsilon = \epsilon_1 - ik_Rt_3 + ik_it_4$. We have introduced the parameters λ_1 and ϵ_1 for the convenience of our calculation.

Using Fourier transform techniques, we may evaluate the space integrals over $\vec{r}$ and $\vec{R}$, respectively. Following real integral form as proposed by Sinha and Sil [40], the three-denominator Lewis integral [41] and applying Cauchy's residual theorem for parameter t_1 and t_4, finally we obtain the

transition amplitude as

$$T_{if} = \frac{2\pi^2 C}{(2\pi i)^2}(2\pi)^{-\frac{9}{2}}\left(\frac{\partial^2}{\partial\lambda\partial\xi_{jk}} - \frac{\partial^2}{\partial\epsilon_1\partial\xi_{jk}}\right) \times \sum_{j=1}^{5}\oint_{\Gamma_2} P(\alpha_2,t_2)dt_2 \oint_{\Gamma_3} P(\alpha_3,t_3)dt_3 \int_0^\infty dy I_C, \quad (11)$$

where

$$I_C = \frac{1}{\alpha'}\left(\frac{\alpha'}{\alpha'+\beta'}\right)^{i\alpha_1}\left(\frac{\alpha'}{\alpha'+\gamma'}\right)^{-i\alpha_4} {}_2F_1[i\alpha_1;-i\alpha_4;1;z]$$

with $z = \frac{\beta'\gamma' - \alpha'\delta'}{(\alpha'+\beta')(\alpha'+\gamma')}$ and ${}_2F_1$ is the hypergeometric function. Here α', β', δ', and γ' are function of the momenta, the velocities, the orbital components of the bound state, and the integration variables (y,t_2,t_3). The original integral occurring in the transition amplitude of Eq. (7) can be described from the present integral I_C by parametric differentiations. The residual three-dimensional integrations t_2, t_3, and y in Eq. (11) are then evaluated numerically [42,43] by using Gauss-Legendre and Gauss-Laguerre quadrature methods. Here our aim is to evaluate the DDCS for the single ionization of polyatomic molecule by proton impact. However, the DDCS for this process integrated over the projectile scattering angle may be obtained [37,44,45] as

$$\frac{d^2\sigma}{dE_e d\Omega_e} = (2\pi)^4\mu^2\frac{k_e}{k_i}\sum_{j=1}^{5}k_R^j\sum_{k=1}^{N}\int |T_{if}|^2 d\Omega_P, \quad (12)$$

where $\mu = A_{\rm ion}M_P$. $A_{\rm ion}$ designates the projectile mass number and M_P is the proton mass. E_e is the energy of the ionized electron. For different values of ϵ_i of each molecular orbital, the scattered proton momenta k_R^j are different. $d\Omega_P$ and $d\Omega_e$ are the differential solid angles of projectile and electron with respect to the direction of incident projectile.

Finally, integration over the projectile scattering angles has been performed numerically with the Gauss-Legendre quadrature method. Convergence of the results has been tested by increasing the number of quadrature points to achieve an accuracy of 0.1%. It is important to note that the wave functions $\chi_{n_{jk}l_{jk}m_{jk}}(\vec{r})$ in Eq. (4) correspond to a particular orientation of the molecular target and can be obtained by applying the rotation operator $D(\alpha,\beta,\gamma)$ [28,46,47] depending on the Euler angles (α,β,γ). Thus, the DDCSs for single ionization of polyatomic molecules are obtained by summing over the five different molecular orbitals.

III. RESULTS AND DISCUSSION

We have computed the DDCS for single ionization of simple polyatomic molecules (CH_4 and NH_3) at incident energies 0.25, 1, and 2 MeV proton impact for fixed electron emission energy using the 3CW model with distortion in the initial state. The variation of DDCS as a function of electron emission angle for fixed emission energy and at different proton impact energies are plotted in Figs. 1–6 for CH_4 and in Figs. 7–11 for NH_3 molecules, respectively. Contributions to DDCS from different orbitals at different proton impact energies have also been analyzed in Figs. 4–6 for CH_4 and in Figs. 10–11 for NH_3,

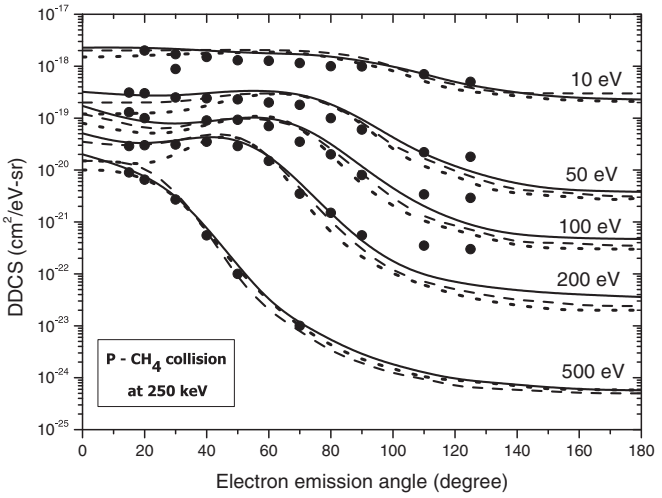

FIG. 1. DDCS for single ionization of CH_4 by 250 keV proton impact as a function of electron emission angle for fixed values of electron energy in eV. Solid curve, present 3CW results; dashed curve, CDW-EIS-MO results [25]; dotted curve, CDW-EIS using Bragg's additivity rule [25]; solid circles, experimental results [49].

respectively. We have calculated the DDCS of single ionization for these systems, which are verified for net ionization with experimental data. For total cross sections (TCSs), the net ionization is obtained by the relation [48], $\sigma_{\rm net} \approx \sigma_1 + 2\sigma_2 + 3\sigma_3$, where σ_1, σ_2, and σ_3 are the single-, double-, and triple-electron ionization cross sections. Here we have applied this approximation in our DDCS calculations.

A. For methane molecule

Theoretical electron angular distributions calculated with the extension of the 3CW model corresponding to the collision between 0.25 MeV H^+ ions and methane molecules, as a function of the electron emission angles from 0° to 180° and for emission energies ϵ_e = 10, 50, 100, 200, and 500 eV,

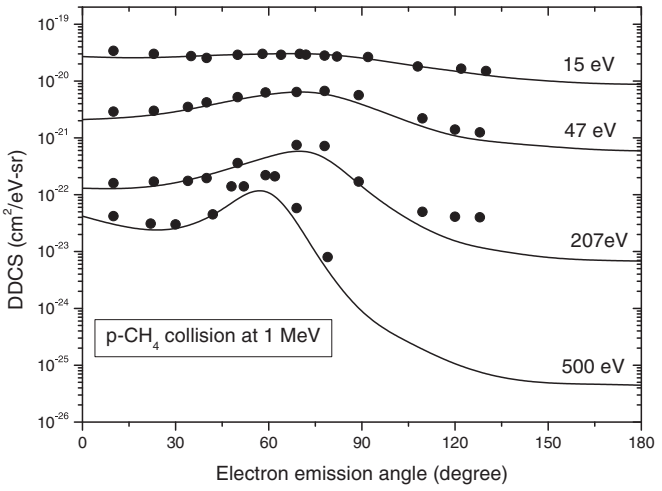

FIG. 2. DDCS for single ionization of CH_4 by 1 MeV proton impact as a function of electron emission angle and for fixed values of electron energy in eV. Solid curve, present 3CW results; solid circles, experimental results [49].

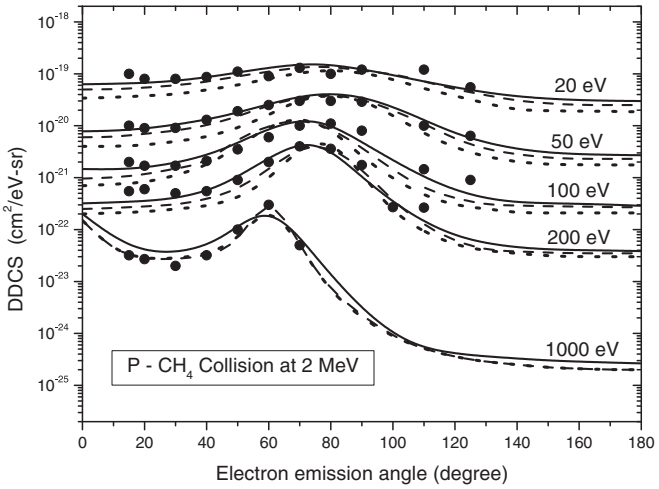

FIG. 3. Same as Fig. 1, but 2 MeV proton impact on CH_4.

respectively, are presented in Fig. 1, together with experimental [24,49] and the other theoretical results [25]. The theoretical results [25] have been obtained by two different approaches: one is called CDW-EIS-MO (dashed curve) where the atomic orbitals is used to construct the molecular orbitals, and the other is Bragg's additivity rule, which is labeled by CDW-EIS (dotted curve). In the CDW-EIS-MO approximation, the ionization DDCS for each molecular orbital has been calculated by taking the linear combination of atomic DDCSs multiplied by coefficients obtained from population analysis, which are given in detail in Ref. [25]. However, in other approaches using Bragg's additivity rule, the DDCS are calculated as the sum of the DDCS corresponding to each atom of the molecule weighted by the number of atom in the molecule.

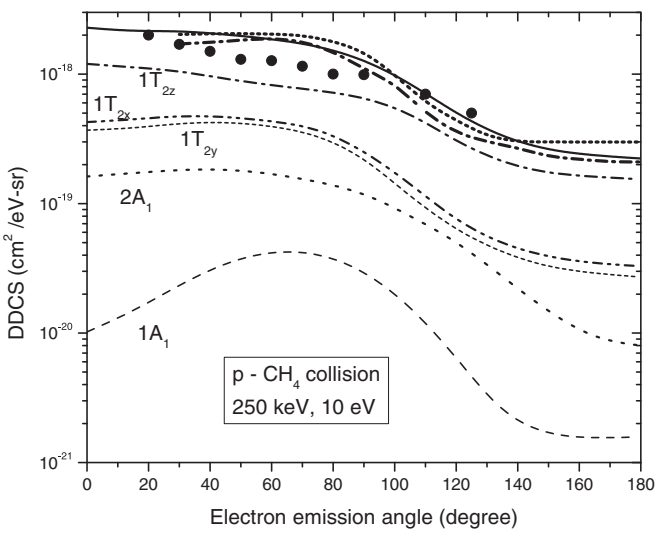

FIG. 4. DDCS molecular orbital contributions for the impact of 250 keV proton on CH_4, as a function of the electron emission angle and for fixed value of the electron emission energy $\epsilon_k = 10$ eV. Solid curve, present results for complete molecule; short dotted curve; CDW-EIS-MO results [25]; short dash-dotted curve, CDW-EIS (Bragg's aditivity rule) [25]; dashed curve, $1A_1$ contribution; dotted curve, $2A_1$ contribution; dash-dot-dotted curve, $1T_{2x}$ contribution; short dashed curve, $1T_{2y}$ contribution; dash-dotted curve, $1T_{2z}$ contribution; solid circles represent experimental results [49].

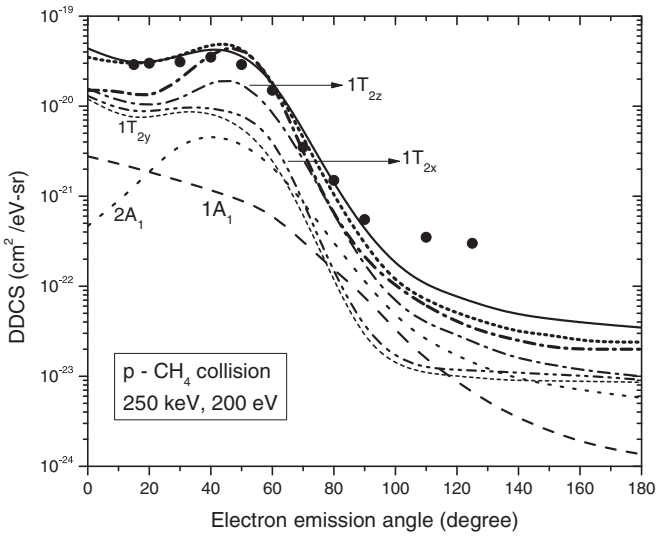

FIG. 5. Same as Fig. 4, but 200 eV electron emission energy.

The present results are found to be in excellent agreement with the experimental results [24,49] at all electron emission energies except at backward angles (above 100°). We find that all theoretical calculations underestimate the experimental data at backward angles, but the present results are in much better agreement with experiment than the other two models (CDW-EIS-MO and CDW-EIS). This behavior at backward angle has also been observed previously for atomic targets. However, it has been shown that it can be corrected by using more accurate wave functions for the initial bound and final continuum states of the target [5,50]. As can be seen from Fig. 1, it is clear that CDW-EIS results using Bragg's additivity rule yield a great discrepancy of results at extreme forward emission angles with increasing electron emission energies. In Fig. 2, we show the DDCS for single

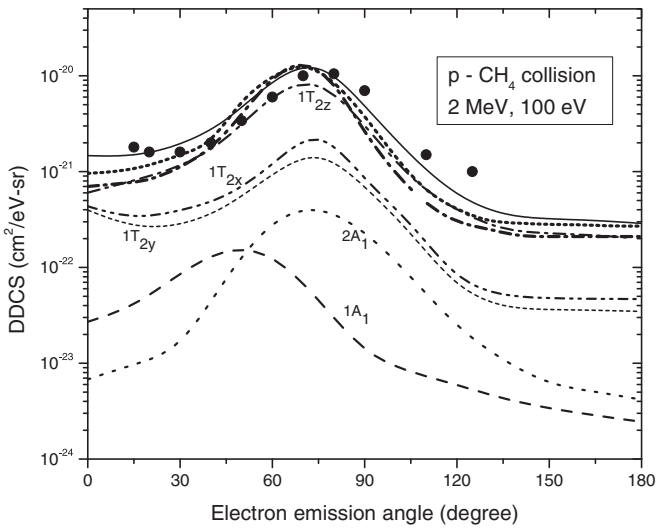

FIG. 6. Same as Fig. 4, but 2 MeV proton impact on CH_4 for 100 eV electron emission energy.

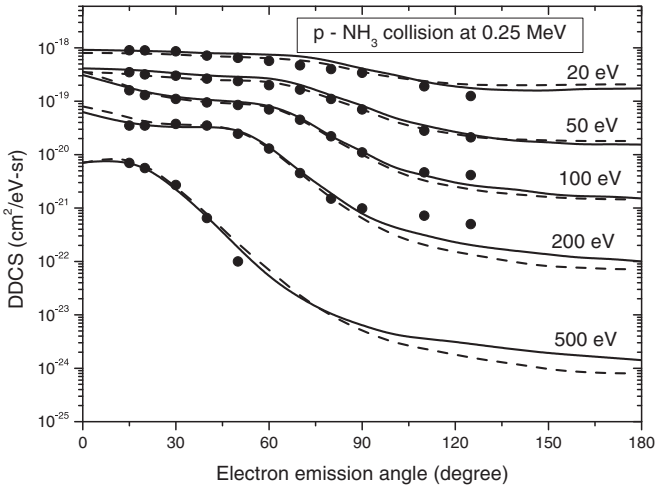

FIG. 7. DDCS for single ionization of NH_3 by the impact of 250 keV proton, as a function of the emission angle and for different electron emission energies. Solid curve corresponds to present results; dashed curve, DDCS-MT results [24]; filled circles represent experimental results [49].

ionization of CH_4 by 1 MeV proton impact. As can be seen from Fig. 2, the agreement between the present theory and only the measurement [49] is very good at electron emission energies of 15 eV and 47 eV in the whole range of emission angles, whereas at 207 eV electron energy, the present results underestimate the experimental data [49] above 100° emission angles. The same behavior is also found in Fig. 1 for 250 keV proton impact.

In Fig. 3, we compare our present results along with the CDW-EIS-MO and CDW-EIS (using Bragg's additivity rule) of Galassi *et al.* [25] with the experimental findings [24] for an incident proton at 2 MeV and for ejected electron energies 20, 50, 100, 200, 1000 eV, respectively. The present results provide overall good agreement within 15–30 % with the

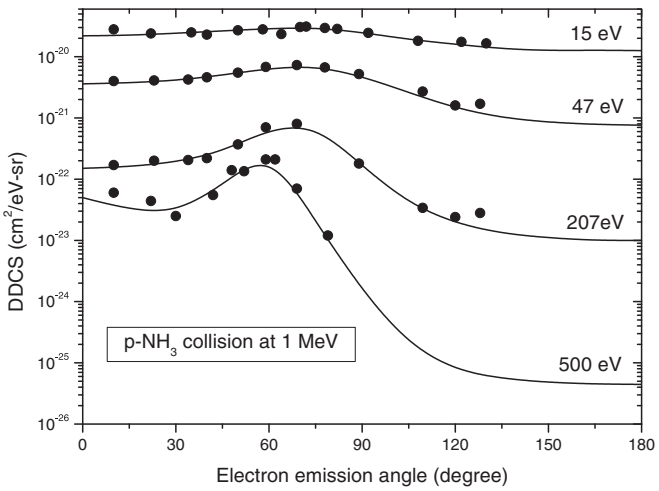

FIG. 8. DDCS for single ionization of NH_3 by 1 MeV proton impact as a function of electron emission angle for fixed values of electron energy in eV. Solid curve, present 3CW results; solid circles represent experimental results [49].

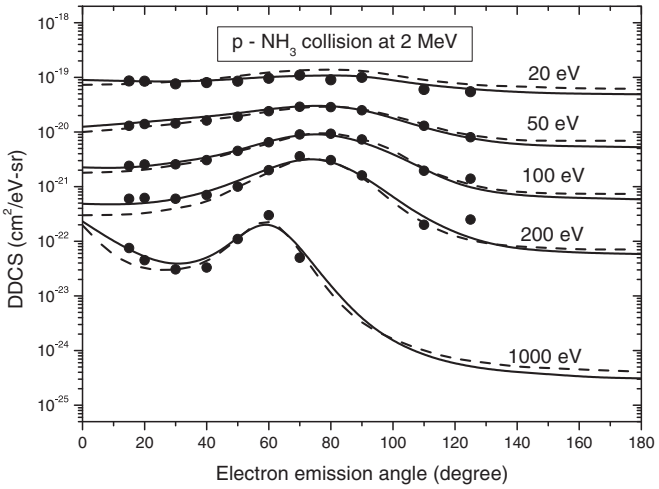

FIG. 9. Same as Fig. 7, but for 2 MeV proton impact on NH_3.

measurement [24] in the whole range of emission angles and at all emission energies except 100 eV and 200 eV, respectively. However, at 100 eV, our results along with other theoretical results underestimate the experimental findings within 20% at the emission angle of 100° and 125°, respectively. This may be due to the choice of the target wave function, which has already been mentioned earlier. We see the enhancement of the DDCS for 500 eV at 1 MeV and 1000 eV at 2 MeV proton at a small angle in all theoretical calculations. This can be explained by the fact that the process of charge transfer to the continuum (ECC), which causes an increase of the DDCS. This process is

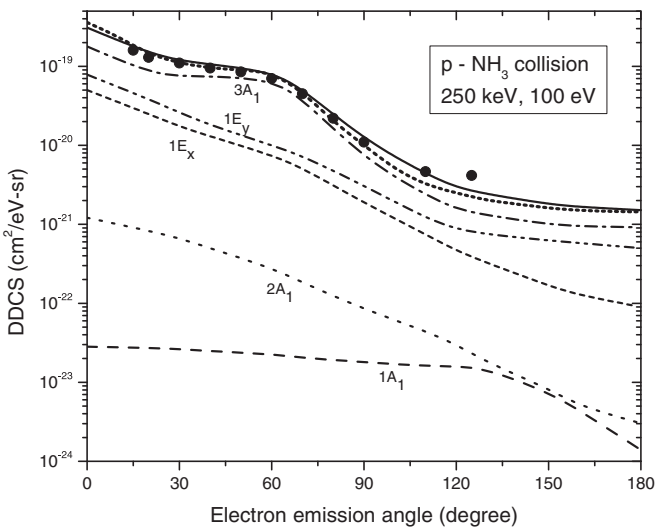

FIG. 10. DDCS molecular orbital contributions for the impact of proton on NH_3, as a function of the electron emission angle and for fixed value of the electron emission energy, $\epsilon_k = 100$ eV at 250 keV proton impact. Solid curve, present results for complete molecule; short dotted curve; CDW-EIS-MO results [25]; short dash-dotted curve, CDW-EIS (Bragg's aditivity rule) [25]; dashed curve, $1A_1$ contribution; dotted curve, $2A_1$ contribution; dash-dot-dotted curve, $1E_x$ contribution; short dashed curve, $1E_y$ contribution; dash-dotted curve, $3A_1$ contribution; solid circles represent experimental results [49].

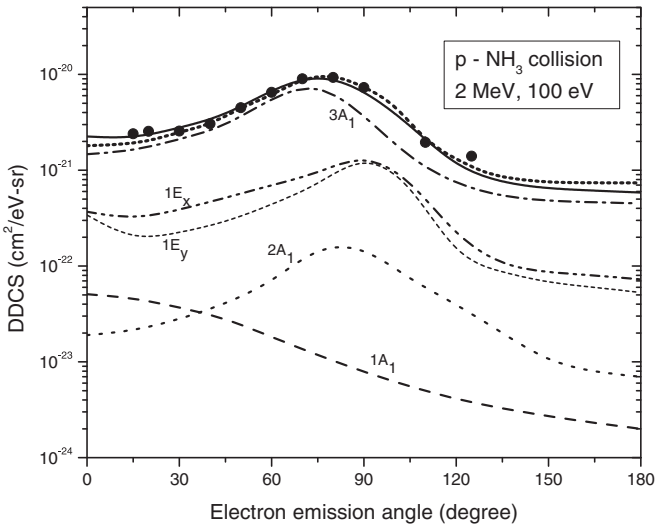

FIG. 11. Same as Fig. 10, but for 2 MeV proton impact on NH_3.

conspicuous when the velocity of the ejected electron is close to those of the scattered proton. This means that an electron is captured from the target molecule into a continuum state of the proton and then emitted in the moving frame of the proton. This effect can also be called the Thomas effect [51], which is a classical picture. In Figs. 1–3, we also find the clear binary peak, which is shifted towards the smaller electron emission angles with increasing electron emission energies. This is due to the decrease of magnitude of relative velocity between the incident proton and ejected electron. The binary peak corresponds to binary collisions in which the energy lost by the incident projectile is completely transferred to the ionizing electron in the molecular target. It is also noted that the present results along with the two sets of CDW-EIS calculation give the identical results at the binary peak.

From Figs. 1–3, we find that the present theoretical DDCS results are in overall good agreement with the experimental results for net ionization. However, the DDCS for single-electron ionization is dominant over double- and triple-electron ionization in this energy range considered. In Figs. 4–6, the contribution of different orbitals to the DDCS is discriminated for the impact of 250 keV proton on methane. The present calculations are presented at 10 eV (in Fig. 4) and 200 eV (in Fig. 5) electron ejection energies. At the lower ejection energy (10 eV), the preference for ionization is ordered according to the initial orbital bonding energy, decreasing the contributions from the lesser bound electrons in the orbitals ($1T_{2z}$, $1T_{2x}$, $1T_{2y}$) to the more bound ($1A_1$ and $2A_1$) ones. At relatively low emission energy at 10 eV shown in Fig. 4, the difference between DDCS results for extreme forward angles and those at extreme backward angles are relatively small. However, as the emission energy increases (200 eV in Fig. 5) such difference at forward and backward angles increases. This forward and backward character has also been observed for different atomic as well as molecular targets [30,31,52–54]. This may be due to the two-center effect (TCE), i.e., the ejected electron moves under the long-range Coulomb field of both projectile and residual target, which is confirmed by other theoretical and experimental findings.

It is observed from Fig. 5 that for higher electron emission energies (200 eV), the DDCS results are slightly dominated by the lightly bound electron ($1A_1$) compared to $2A_1$ at extreme forward angles. This behavior may be explained by the fact that high-energy electron emission is preferable from the inner orbital, which has already been mentioned by Tachino *et al.* [55]. In Fig. 6, the present DDCS for the same collision systems as presented in Figs. 4–5, but for 2 MeV proton energy, are plotted. It can be seen that the present results are better than the two sets of the CDW-EIS model in the region of extreme forward and backward emission angles, i.e., our results along with two sets of CDW-EIS models fail to reproduce the experimental results at extreme backward angles. This reason has already been mentioned earlier. At extreme forward angle, the strongly bound orbitals have significant contribution to the total DDCS results, which is also observed in Fig. 5. As can be seen from Fig. 6, a clear binary peak around 75° (θ_e^P) is observed in different orbitals except for the $1A_1$ orbital, which has been verified by the relation obtained from momentum conservation

$$|\vec{q}| = |\vec{k}_i - \vec{k}_R| = |\vec{k}_e| \Leftrightarrow \theta_e^P = \cos^{-1}\left[\frac{k_i^2 + k_e^2 - k_R^2}{2k_i k_e}\right],$$

where $\vec{q}$ represents the momentum transfer. However, this quantity depends on the ionized molecular orbital j via the dependence on the binding energy of the molecular orbitals.

B. For ammonia molecule

In Fig. 7, theoretical and experimental DDCS for ionization of NH_3 by impact of 250 keV proton are shown as a function of the electron emission angles at fixed electron emission energies. As can be observed, the present results along with DDCS-MT [24] underestimates the experimental data in the small range of emission angles from 100° to 120° at 200 eV electron emission energies. The reason has already been mentioned earlier. However, overall agreement between the present results and experimental findings are excellent in the whole electron emission angles and for all electron emission energies. From Fig. 7, we find that the other model prescribed by Senger *et al.* [56] gives almost the same value except at high emission angles and high emission energies. In this model, Senger *et al.* have expressed the DDCS in terms of generalized oscillator strength and treated the multielectronic diatomic or polyatomic molecule as a two-body system comprising the active electron and the residual target ion. They have described it as DDCS with mixed treatment and abbreviated it as DDCS-MT. For the same collision process, we have also plotted the DDCS as a function of emission angles for different electron energies at 1 MeV proton impact in Fig. 8. The present data are only compared with the existing experimental results [49]. The figure shows that the present calculated results agree very well with experiment [49].

In Fig. 9, we have plotted the same at 2 MeV proton impact. The structure of our calculated DDCS results and the results obtained using the DDCS-MT model agree very well with the measured data. We also observe the binary peak, which shifts towards lower emission angle with increasing emission energy. At extreme forward angle and for high emission energy the ECC effect is observed. These features

have also been observed in p-CH_4 collision at 1 MeV and 2 MeV (in Fig. 2 and Fig. 3). In comparison of our present results with experimental data, we see from Fig. 3 for CH_4 and Fig. 9 for NH_3 that the discrepancies have been found for p-CH_4 collision at 2 MeV in the region of small electron emission angles with increasing electron emission energies. DDCS molecular orbital contributions for the impact of 250 keV and 2 MeV proton on NH_3 as a function of the electron emission angle and for fixed value of the electron emission energy (100 eV) are shown in Figs. 10–11. From these figures, we see that the contributions of DDCS from the less bound electrons is dominant over strongly bound electrons. The same feature is also observed in Fig. 5.

It is observed from Fig. 6 and Fig. 11 that the DDCS results for extreme forward angles and those at extreme backward angles are relatively close to each other. However, the two-center effect is negligible at high projectile energy and at low electron emission energy. In comparison between CH_4 and NH_3 molecules by the impact of proton at 1 MeV (in Fig. 2 and in Fig. 8), the DDCS result around binary peak for a fixed electron emission energy (say 200 eV) is slightly greater in NH_3 than CH_4 within 10–20 %, whereas at 2 MeV (in Fig. 3 and Fig. 9), the same for CH_4 dominates over NH_3 within 15–30 %. This is justified because at the high impact energies, the charged projectile can penetrate more easily in the region of the core orbitals of CH_4 than NH_3.

IV. CONCLUSIONS

The single-electron ionization of CH_4 and NH_3 induced by 0.25, 1, and 2 MeV proton beams has been theoretically investigated here by means of the extended three-coulomb wave model within an independent particle model where only one electron is considered as active. This approach allowed us to reduce the complexity of such multielectronic systems to simpler monoelectronic ones. Moreover, the molecular orbitals of simple polyatomic molecular targets investigated here are described by linear combinations of atomic orbitals with Slater-basis sets. We discussed the contributions to DDCS from different molecular orbitals. The maximum contributions to DDCS for single ionization comes from the less bound electrons in respective orbitals, whereas the tightly bound electrons dominate the DDCS at extreme forward emission angles at a high projectile energy and for a fixed electron emission energy. Moreover, the forward-backward angular asymmetry in DDCS spectrum due to two-center effect (TCE) is not observed at 100 eV both for CH_4 and NH_3 target when the projectile energy is high.

It is clear that the CDW-EIS calculation using Bragg's additivity rule gives unsatisfactory results at intermediate projectile energy. This is clear evidence for the applicability of the rule at this energy. From the investigation of simple polyatomic molecules, we see that the success of an approximate method depends on the inclusion of the dynamical features of collisions. In this respect, present model is quite successful in achieving good agreement with experiments at high impact energy, except at backward emission angles. However, more investigations are required for other charge states and energies of the incoming projectile to test the validity of the present theoretical investigation.

ACKNOWLEDGMENT

The authors gratefully acknowledge the financial support from the SERB, New Delhi, India under Grant No. SB/S9/LOP-0009/2013.

[1] N. Stolterfoht, R. D. Dubois, and R. D. Rivarola, *Electron Emission in Heavy Ion-Atom Collisions* (Springer, New York, 1997).
[2] U. Amaldi and G. Kraft, Rep. Prog. Phys. **68**, 1861 (2005).
[3] P. D. Fainstein, V. H. Ponce, and R. D. Rivarola, J. Phys. B: At. Mol. Opt. Phys. **21**, 287 (1988).
[4] P. D. Fainstein, L. Gulyas, F. Martin, and A. Salin, Phys. Rev. A **53**, 3243 (1996).
[5] L. Gulyas, P. D. Fainstein, and A. Salin, J. Phys. B: At. Mol. Opt. Phys. **28**, 245 (1995).
[6] L. C. Tribedi, P. Richard, L. Gulyas, M. E. Rudd, and R. Moshammer, Phys. Rev. A **63**, 062723 (2001).
[7] L. C. Tribedi, P. Richard, W. Deltaven, L. Gulyas, M. W. Gealy, and M. E. Rudd, J. Phys. B: At. Mol. Opt. Phys. **31**, L369 (1998).
[8] J. M. Frisch *et al.*, *Gaussian 09 Revision A-I* (Gaussian Inc., Wallingford, 1999).
[9] W. J. Hehre, R. F. Stewart, and J. A. Pople, J. Chem. Phys. **51**, 2657 (1969).
[10] M. Moccia, J. Chem. Phys. **40**, 2186 (1964).
[11] M. Murakami, T. Kirchner, M. Horbatsch, and H. J. Lüdde, Phys. Rev. A **85**, 052704 (2012).
[12] L. F. Errea, C. Illescas, L. Méndez, and I. Rabadán, Phys. Rev. A **87**, 032709 (2013).
[13] A. Salehzadeh and T. Kirchner, Eur. Phys. J. D **71**, 66 (2017).
[14] C. M. Granados-Castro and L. U. Ancarani, Eur. Phys. J. D **71**, 65 (2017).
[15] C. C. Montanari and J. E. Miraglia, J. Phys. B: At. Mol. Opt. Phys. **47**, 015201 (2014).
[16] M. Brauner, J. S. Briggs, and H. Klar, J. Phys. B: At. Mol. Opt. Phys. **22**, 2265 (1989).
[17] I. Bray and A. T. Stelbovies, Adv. At. Mol. Opt. Phys. **35**, 209 (1995).
[18] M. Baertschy, T. N. Rescigno, W. A. Isaacs, X. Li, and C. W. McCurdy, Phys. Rev. A **63**, 022712 (2001).
[19] S. Nandi, S. Biswas, A. Khan, J. M. Monti, C. A. Tachino, R. D. Rivarola, D. Misra, and L. C. Tribedi, Phys. Rev. A **87**, 052710 (2013).
[20] R. Moccia, J. Chem. Phys. **40**, 2164 (1964).
[21] R. Moccia, J. Chem. Phys. **40**, 2176 (1964).
[22] R. G. A. R. Maclagan, Aust. J. Chem **28**, 927 (1975).
[23] C. Champion, Phys. Med. Biol. **55**, 11 (2010).
[24] B. Senger, Z. Phys. D: At. Mol. Clusters **9**, 79 (1988).
[25] M. E. Galassi, R. D. Rivarola, M. Beuve, G. H. Olivera, and P. D. Fainstein, Phys. Rev. A **62**, 022701 (2000).
[26] G. H. Olivera, A. E. Martinez, R. D. Rivarola, and P. D. Fainsteins, Radiant. Res. **144**, 241 (1995).

[27] B. Senger and R. V. Rechenmann, Nucl. Instrum. Methods Phys. Res B. **2**, 204 (1984).
[28] C. Champion, J. Hanssen, and P. A. Hervieux, J. Chem. Phys. **121**, 9423 (2004).
[29] M. A. Bolorizadeh and M. E. Rudd, Phys. Rev A. **33**, 882 (1986).
[30] C. Dal Cappello, P. A. Hervieux, I. Charpentier, and F. Ruiz-Lopez, Phys. Rev. A **78**, 042702 (2008).
[31] O. Boudrioua, C. Champion, C. Dal Cappello, and Y. V. Popov, Phys. Rev. A **75**, 022720 (2007).
[32] L. Fernández-Menchero and S. Otranto, Phys. Rev. A **82**, 022712 (2010).
[33] L. Gulyas, I. Toth, and L. Nagy, J. Phys. B: At. Mol. Opt. Phys **46**, 075201 (2013).
[34] M. Yavuz, Z. N. Ozer, M. Ulu, C. Champion, and M. Dogan, J. Chem. Phys. **144**, 164305 (2016).
[35] C. A. Tachino, J. M. Monti, O. A. Fojon, C. Champion, and R. D. Rivarola, J. Phys.: Conf. Ser. **583**, 012020 (2015).
[36] A. Mondal, C. R. Mandal, and M. Purkait, Eur. Phys. J. D **70**, 16 (2016).
[37] A. Mondal, C. R. Mandal, and M. Purkait, J. Phys. B: At. Mol. Opt. Phys. **49**, 075201 (2016).
[38] M. J. Brothers and R. A. Bonham, J. Phys. B **17**, 4235 (1984).
[39] A. Nordsieck, Phys. Rev. **93**, 785 (1954).
[40] C. Sinha and N. C. Sil, J. Phys. B **11**, L333 (1978).
[41] R. R. Lewis, Phys. Rev. **102**, 537 (1956).
[42] R. Biswas and C. Sinha, Phys. Rev. A. **50**, 354 (1994).
[43] S. Jana, C. R. Mandal, and M. Purkait, J. Phys. B: At. Mol. Opt. Phys. **48**, 045203 (2015).
[44] H. L. Champion, M. E. Galassi, O. Fojon, R. D. Rivarola, and J. Hassen, Phys. Med. Biol **55**, 6053 (2010).
[45] A. Mondal, C. R. Mandal, and M. Purkait, Nucl. Instrum. Method. Phys. Res. B **353**, 28 (2015).
[46] C. Champion, J. Hanssen, and P. A. Hervieux, Phys. Rev. A. **63**, 052720 (2001).
[47] A. Messiah, *Quantum Mechanics Vol 2* (North-Holland, Amsterdam, 1962).
[48] T. Kirchner, L. Gulyas, H. J. Ludde, E. Engel, and R. M. Dreizler, Phys. Rev. A. **58**, 2063 (1998).
[49] D. J. Lynch, L. H. Toburen, and W. E. Wilson, J. Chem. Phys **64**, 2616 (1976).
[50] D. H. Madison, Phys. Rev. A **8**, 2449 (1973).
[51] L. H. Thomas, Proc. R. Soc. London, Ser. A **114**, 561 (1927).
[52] L. Gulyas and P. D. Fainstein, J. Phys. B: At. Mol. Opt. Phys **31**, 3297 (1998).
[53] S. Jana, R. Samanta, and M. Purkait, Eur. Phys. J. D **66**, 243 (2012).
[54] S. Jana, R. Samanta, and M. Purkait, Phys. Scr. **88**, 055301 (2013).
[55] C. A. Tachino, J. M. Monti, O. A. Fojon, C. Champion, and R. D. Rivarola, J. Phys. B: At. Mol. Opt. Phys **47**, 035203 (2014).
[56] R. Senger, E. Wittendorp, and R. V. Rechenmenn, Nucl. Instrum. Methods **194**, 437 (1982).